# Stability Analysis of Nonlinear Current-Sharing Techniques

David J. Perreault  John G. Kassakian  George C. Verghese

Massachusetts Institute of Technology
Laboratory for Electromagnetic and Electronic Systems
Cambridge, MA 02139 USA

*Abstract* - **This paper addresses the dynamic analysis of paralleled power converter systems employing nonlinear load-sharing control techniques. The first section of the paper analyzes nonlinear load-sharing control techniques which are linearizable about a constant operating point. The second section of the paper analyzes the dynamics of the widely-used UC3907 control scheme for an important special case. In both cases, the analyses are validated against experimental results.**

## I. Introduction

Power converters are often paralleled to achieve a high system rating or improve system reliability. One desirable characteristic of a parallel converter system is for the individual converters to share the load current equally and stably, in order to reduce the converter stresses and improve system reliability. Active control techniques are often employed to achieve load sharing while retaining good regulation of the output voltage [1-17]. The ability to accurately predict load-sharing stability and system dynamics is thus an important aspect of the design of a parallel power converter system, and has been the subject of recent attention [8,10,15-17]. However, all of these analyses focus on linear feedback control methods, and are based on feeding back either the average current output of the cells or the current of a designated "master" cell. While these are important cases, many distributed load-sharing control methods, including those introduced in [6,7,12-14], use feedback based on other quantities, and have inherently nonlinear dynamics. This paper addresses the dynamic analysis of systems employing nonlinear load-sharing control techniques, and validates these analyses against experimental results. Section II analyzes nonlinear load-balancing control methods which are linearizable about a constant operating point. This follows the approach of a recently-developed analysis of the linear feedback case [15,16], but explicitly considers the linearization of nonlinear current-sharing control laws. Section III applies this approach to the frequency-based current-sharing control scheme developed in [12-14], and compares the analytical predictions to experimental results. Section IV considers a widely-used nonlinear feedback control scheme which is not easily handled by linearization in the general case [7], and identifies conditions under which it is easily analyzed. Section V analyzes an example system and validates this analysis against experimental results.

## II. Small-Signal Analysis

Here we address the dynamic analysis of an $N$-cell, dc-output parallel converter system about a fixed operating point. As shown in Fig. 1, we model the $j^{th}$ cell as a voltage source $v_{r,j}$ (equal to the cell reference voltage) in series with an output impedance $Z_j$, while the load is modeled as an impedance $Z_L$. The load-sharing controllers, which operate by adjusting the reference voltages according to the load-balance condition, have nonlinear dynamics

$$\frac{dv_{r,j}}{dt} = g_j(v_{r,j}, i_1, \ldots, i_N) \quad for \quad j \in [1, \ldots, N] \; . \tag{1}$$

We consider the dynamic behavior of such a system about a fixed operating point where

$$g_j(V_{r,j}, I_1, \ldots, I_N) = 0 \quad for \quad j \in [1, N] \; . \tag{2}$$

The functions $g_j(\bullet)$ are assumed to have continuous first derivatives at the operating point, allowing the operating point stability and small-signal dynamics to be determined using Liapunov's indirect method (i.e. linearization). The linearized system dynamics are determined by considering the behavior of small perturbations such that:

$$\begin{aligned} i_j &= I_j + \hat{i}_j \quad for \quad j \in [1, N] \\ v_{r,j} &= V_{r,j} + \hat{v}_{r,j} \quad for \quad j \in [1, N] \end{aligned} \tag{3}$$

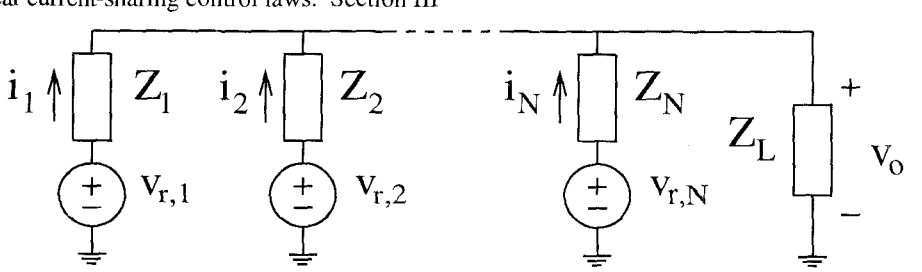


**Figure 1** A model for an $N$-cell parallel converter system driving a load impedance $Z_L$.

0-7803-3840-5/97/$10.00 © 1997 IEEE

Expanding the equations **(1)** in a Taylor series about the operating point **(2)** and neglecting higher order terms, we find

$$\begin{aligned} \frac{d\hat{v}_{r,j}}{dt} &= \frac{\partial g_j}{\partial v_{r,j}}\hat{v}_{r,j} + \frac{\partial g_j}{\partial i_1}\hat{i}_1 + \cdots + \frac{\partial g_j}{\partial i_N}\hat{i}_N \\ &= J_{j0}\cdot\hat{v}_{r,j} + J_{j1}\cdot\hat{i}_1 + \cdots + J_{jN}\cdot\hat{i}_N \end{aligned} \quad (4)$$

where the partial derivatives are evaluated at the operating point.

Proceeding from the linear equations **(4)**, the approach outlined in [16] can be directly employed to analyze the dynamics of the system. For the case where each cell treats all other cells identically (i.e., where the functions $g_j(\bullet)$ are symmetric with respect to the currents of the other cells), we may write

$$J_{jl} = J_{j*} \quad \forall \quad l \neq 0, j \,, \quad (5)$$

and find the characteristic polynomial of the system as the numerator of

$$\left(1 + \sum_{j=1}^{N} \frac{(s - J_{j0})Z_L - J_{j*}}{(s - J_{j0})Z_j + J_{j*} - J_{jj}}\right) \cdot \left(\prod_{k=1}^{N} [(s - J_{k0})Z_k + J_{k*} - J_{kk}]\right) = 0 \,. \quad (6)$$

The stability and dynamics of the system can be found by solving for the roots of the characteristic polynomial, or through the use of other stability criteria.

## III. Application Example

To illustrate the application of this analysis technique and demonstrate its validity experimentally, we consider the nonlinear frequency-based current-sharing technique developed in [12-14]. In this technique, each cell generates a signal whose frequency is related to its output current. The cells are able to calculate the root-mean-square of the generated frequencies. Each cell has a load-sharing controller which adjusts the local voltage reference based on the difference between its own generated frequency and the rms frequency in order to achieve load sharing. One benefit of this frequency-based load-sharing method is that it can be implemented without any additional interconnections among converters.

Here we analyze a two-cell buck converter system of the type described in [13,14], and compare the analytical predictions to experimental results. We begin by developing a model for the system in the form of Fig. 1, and then proceed to analyze the current-sharing dynamics of the system.

We model each converter cell as a voltage source equal to the cell reference voltage, in series with an output impedance. The appropriate output impedance can be determined by examining the cell control characteristics. Each cell has a voltage control loop that operates with the current-mode-controlled power stage to generate a cell output current that depends on the error between the output voltage and the local reference voltage. The voltage control compensator used in the prototype system yields a transfer function from error voltage $v_{err}$ to cell output current $i_{out}$ of

$$\frac{i_{out}}{v_{err}}(s) = \frac{125}{0.18s + 1} \quad \frac{mA}{V} \quad (7)$$

which corresponds to a cell output impedance of

$$Z_j(s) = \frac{0.18s + 1}{125} \quad \frac{V}{mA} \,. \quad (8)$$

This cell output impedance, which can be represented as the series combination of a resistor (8 Ω) and an inductor (1.42 H), appears in series with each cell's reference voltage in the model of Fig. 1. The parallel combination of the filter capacitance and load resistance forms a load impedance

$$Z_L = \frac{R_L}{sC_f R_L + 1} \quad (9)$$

which completes the model of Fig 1.

We now analyze the current-sharing control mechanism used in the prototype system. To achieve current-sharing, each cell in the prototype system encodes information about its output current in the frequency of an output perturbation signal, and adjusts its reference voltage based on the difference between its own perturbation frequency and the rms of the two perturbation frequencies. The frequencies generated by the cells are related to their output currents in the following manner:

$$\begin{aligned} f_1 &= a + bi_1 \\ f_2 &= a + bi_2 \end{aligned} \quad (10)$$

with $a = 5$ kHz and $b = 0.2$ kHz/mA for the prototype system. In the control circuitry of the prototype system, frequency values are represented as voltages using a scaling factor of 1 V/kHz. Expressing frequency values in **(10)** in terms of their equivalent voltages yields the representation:

$$\begin{aligned} v_{\omega,1} &= a' + b'i_1 \\ v_{\omega,2} &= a' + b'i_2 \end{aligned} \quad (11)$$

where $a' = 5$ V, and $b' = 0.2$ V/mA.

Each cell computes an estimate of the rms of the individual perturbation frequencies. Neglecting the dynamics of the estimation process, and expressing frequency values in terms of equivalent voltages, the rms frequency estimate can be expressed as

$$v_{\omega,est} \simeq \sqrt{\frac{v_{\omega,1}^2 + v_{\omega,2}^2}{2}} \,. \quad (12)$$

Current-sharing is achieved in the experimental system by adjusting the local cell reference voltages within limits about a base value $V_{r,base}$. Each cell has a high-gain, single-pole compensator that generates the adjustment $\Delta v_r$ based on the difference between the local cell perturbation frequency $v_{\omega,pert}$ (equal to $v_{\omega k}$ for the $k^{th}$ cell) and the estimated rms frequency $v_{\omega,est}$. The differential equation describing the adjustment of the local

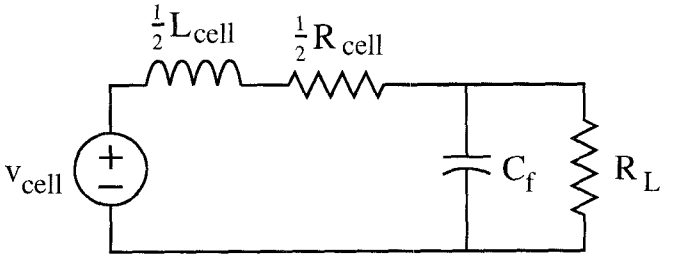


**Figure 2** A common-mode model for the dynamics of a two-cell system.

cell reference voltage is

$$\frac{d\Delta v_r}{dt} = C_A(v_{\omega,est} - v_{\omega,pert}) - C_B\Delta v_r \cong 0.3(v_{\omega,est} - v_{\omega,pert}) - 0.03\Delta v_r \quad \textbf{(13)}$$

which may also be expressed in the form

$$\frac{d\Delta v_r}{dt} = g(\Delta v_r, i_1, i_2) \quad \textbf{(14)}$$

using the relations **(11)** and **(12)**. Computing the partial derivatives in the expansion **(4)**, we find

$$\begin{aligned} J_{10} &= J_{20} = -C_B \approx -0.03 \text{ sec}^{-1} \\ J_{11} &= J_{22} = -\tfrac{1}{2}bC_A \approx -0.03 \text{ V/mA} \\ J_{12} &= J_{21} = \tfrac{1}{2}bC_A \approx 0.03 \text{ V/mA} \end{aligned} \quad \textbf{(15)}$$

for perturbations away from steady-state operating points where $I_1 = I_2$. From **(6)** we find the characteristic polynomial for this system to be

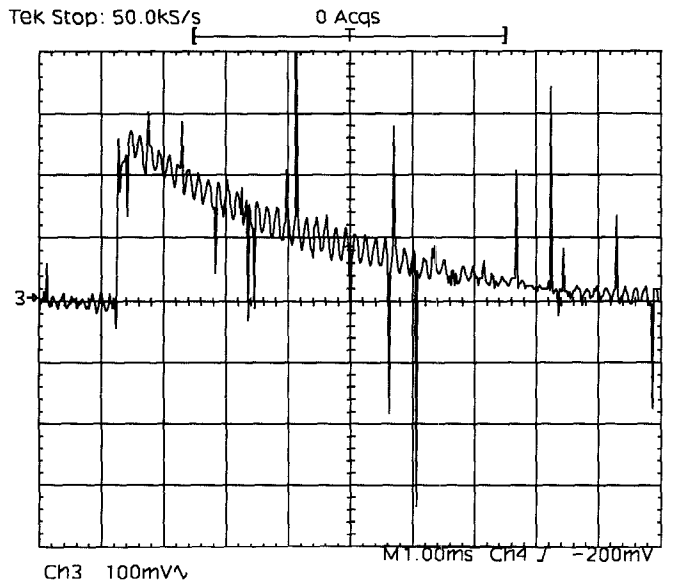


**Figure 3** Voltage response of the two-cell experimental system to a load step from 349 Ω to 390 Ω.

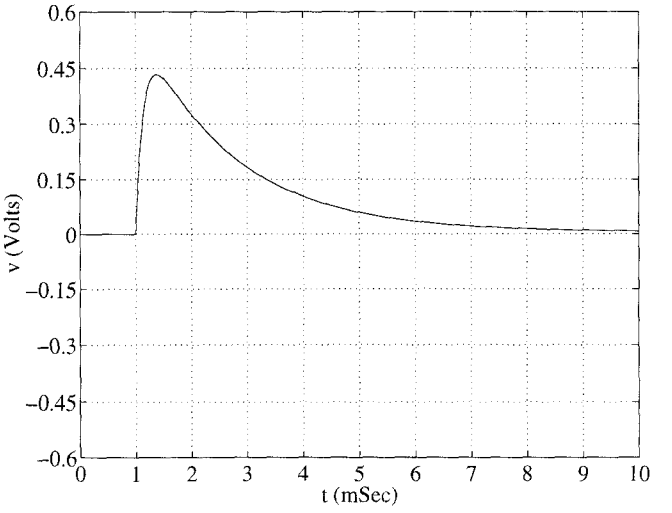


**Figure 4** Response of the single-cell "common-mode" model to a step in load from 349 Ω to 390 Ω. This response has poles at $s$ = -557 and $s$ = -7639.

$$(s + 556.9)(s + 7638.6)(s + 0.03)\cdot (s + 2.79 + j5.83)(s + 2.79 - j5.83) = 0. \quad \textbf{(16)}$$

We now compare the dynamics predicted by **(16)** to the behavior of the experimental system. The first two poles in **(16)** match those of a single-cell system in which the single cell has a fixed reference voltage and exactly half of the output impedance of the cells in the two-cell system (Fig. 2). These poles thus correspond to the common-mode response of the two cells to disturbances in the output voltage. Figure 3 shows the output voltage response to a load step from 349 Ω to 390 Ω. The transient response is composed of a voltage increase with a fast time constant, followed by a decay at a slower time constant. (The small, high-frequency ripple in the output voltage is a perturbation component used to carry current-sharing information in the experimental system.) For comparison, Fig. 4 shows the ac response to a similar load step of the common mode model of Fig. 2, which has pole locations matching the two leftmost factors in **(16)**. From the similarity of the rise and fall times seen in figures 3 and 4, we conclude that **(16)** predicts the common-mode dynamic behavior of the experimental system to within reasonable experimental accuracy.

The remaining three pole locations in **(16)** describe the dynamics of the reference adjustment and current-sharing process. Figure 5 shows the reference current response of the cells during a large-signal transient induced by making electrical connections that disturbed the cell reference voltages. During this transient, the output voltage remained relatively unchanged, while the swings in current sharing occurred as the current-sharing control loops adjusted the reference voltages to re-establish current

sharing. Based on the natural frequency and the damping ratio, the observed time response matches that of a system with a zero at $s = 0$ and poles at $s = -2.9 \pm j5.0$. This corresponds reasonably well to the pole pair predicted at $s = -2.8 \pm j5.8$ by the linearized analysis, especially given the large-signal nature of the transient.

Behavior associated with the remaining pole predicted by the linearized analysis was also sometimes observed after the reference voltages were disturbed, especially when the disturbance was severe. After such a disturbance, a small, very slow adjustment of the output voltage (and cell currents) to a final steady-state value could sometimes be observed, typically ending with the reference voltages near the edge of their adjustment range. When observed, this adjustment took as much as twenty or more seconds to complete, with an approximately linear transition to a final value. This behavior matches that of a slow first-order response which saturates before reaching its final value (due to the clamping of the reference voltage adjustments), and is at least qualitatively consistent with the pole at $s = -0.03$ predicted by the linearized analysis.

What may be concluded from these results is that the presented approach allows prediction of system stability and dynamics about an operating point for nonlinear feedback control laws which are linearizable. This is useful, since many load-sharing control methods rely on such nonlinear feedback control laws.

## IV. Analysis of the UC3907 Method

While the preceding analysis is useful for a broad range of load-sharing control methods, others are not amenable to this approach due to the difficulty of linearizing the system or due to the limited range of perturbations for which the linearized analysis is accurate. One widely-used load-sharing method which is not easily handled by linearization is the peak-current control scheme implemented the UC3907 load-sharing control IC [7]. Small-signal dynamic analyses of the master-slave current-sharing technique (in which the local cells compare their currents to that of a designated master) are sometimes employed to predict the behavior of the peak-current control scheme of the UC3907[16,17]. However, in the UC3907 method, the cell carrying the highest current cell acts as master, and the master designation can switch dynamically among cells under current-sharing perturbations of just a few percent. This can lead to behavior not predicted by these analyses. This section will establish an important special case in which the master cannot switch, thus allowing the system to be easily analyzed.

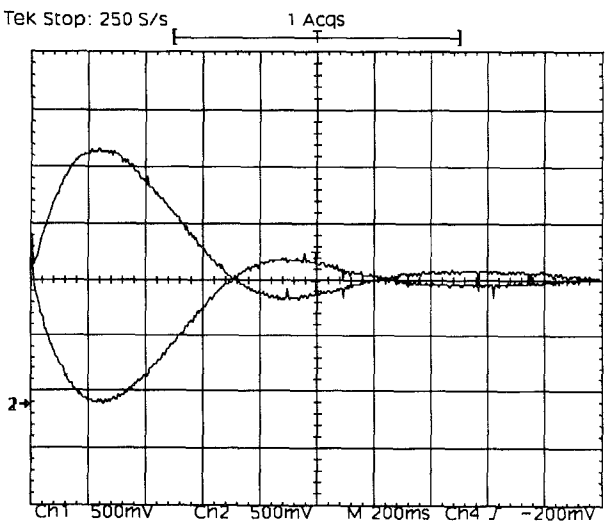


**Figure 5** Dynamic response of the cell reference currents to a disturbance of the reference voltages in the two-cell experimental system while operating at a load resistance of 390 Ω.

The load-sharing control scheme implemented in the UC3907 operates as follows: Each cell shifts its own voltage reference via integral control, based on the difference between its own output current and the maximum output current of all the cells minus a small offset. Thus,

$$\frac{dv_{r,j}}{dt} = \begin{cases} K_j[i_{\max} - \Delta I - i_j] & for \quad v_{r,j,base} < v_{r,j} < v_{r,j,\max} \\ 0 & otherwise \end{cases} \tag{17}$$

where $K_j$ and $i_j$ are the (integral) control gain and output current of the $j^{th}$ cell, $i_{max}$ is the maximum output current of all of the cells, and $\Delta I$ is a small offset. The $j^{th}$ reference is adjustable over a small range from a base value $v_{r,j,base}$ to a maximum value $v_{r,j,max}$, and is prevented from going outside of this range by clamping of the reference at the boundaries. The offset $\Delta I$ ensures that the highest-current cell will carry slightly more current than the other cells under static conditions, thus preventing the maximum current signal from chattering among different cell currents. The offset also guarantees that the voltage reference of the highest-current cell will always be driven towards its base value.

We will consider the case where the output impedances of the cells are resistive. This is typical of current-mode controlled converters under proportional control, for example. We will first analyze the case where the cell output resistances are constant, and then discuss the changes that occur when the output resistances vary with load. We will also make the simplifying assumption that all the cells are identical except for their references and current-sharing control gains. That is, it is assumed that the cells all have identical output impedances, sensor gains, etc. While these assumptions are somewhat limiting, they are still reasonable for many cases of practical interest.

We first consider the case in which the cell output impedances are constant across load. As illustrated in Fig. 1, we model the $j^{th}$ cell as a voltage source $v_{r,j}$ (equal to the reference voltage) in series with a cell output impedance $R_j = G_j^{-1}$. The $j^{th}$ cell thus has output current

$$i_j = G_j[v_{r,j} - v_o] \ . \tag{18}$$

For the considered case of identical and constant cell output admittances ($G_1 = \cdots = G_N = G_{out}$), a cell with a higher reference voltage always carries more current than a cell with a lower reference voltage. We will assume without loss of generality that the $N^{th}$ cell has the highest base reference voltage. Because the offset $\Delta I$ always drives the highest current cell's reference towards its base value, within a short time after startup the $N^{th}$ cell will have the highest reference voltage and output current.

Using **(24)**, we can express the sensitivity of differences in cell currents to changes in output voltage as

$$\frac{\partial}{\partial v_o}[i_j - i_k] = G_j - G_k \,. \qquad \textbf{(19)}$$

It may be inferred from this equation that for the case of identical output impedances, differences between the cell currents do not depend on the output voltage. This means that the $N^{th}$ cell will carry the highest current permanently, regardless of changes in output voltage (yielding $i_{max} = I_N$). Under this condition, the control scheme is easily analyzed using frequency-domain techniques already developed for Master-Slave current sharing control [16,17], or through time-domain analysis. (One slight difference between the UC3907 control law **(17)** and the forms used in **(1)** or in [16] is the existence of the constant term $\Delta I$. However, this element is easily accommodated, and does not affect the resulting natural frequencies.) Furthermore, due to the structure of the control law **(17)**, the reference voltage adjustment process is not influenced by changes in output voltage.

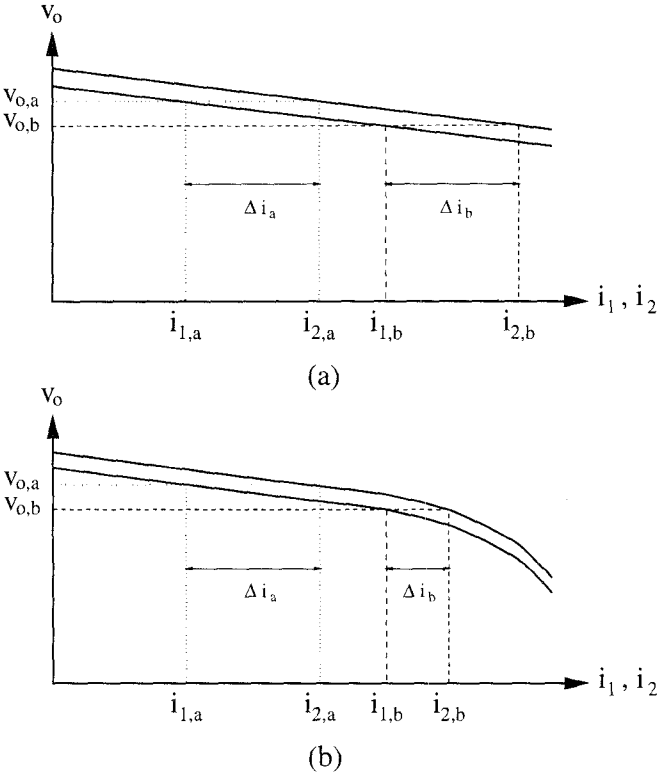


**Figure 6** Load-line diagrams illustrating current-sharing behavior for a two-cell system. (a) Constant cell output resistances. (b) Load-varying cell output resistances.

Information about the large-signal behavior of the system can also be inferred in this case. The reference voltage of the maximum-current cell (the $N^{th}$ cell) is always "frozen" at its base value during operation. Consider what happens when any other cell reaches one of its adjustment boundaries (and thus momentarily ceases to change). Both that cell's current and the $N^{th}$ cell's current are then only affected by the output voltage, and the difference between the two cell currents is not affected by output voltage. As a result, there is no mechanism for the current-sharing error (which initially drove the cell's reference to the boundary) to change, and the reference of that cell will remain permanently frozen there. Similarly, if the error term in **(17)** driving the reference change of a cell reaches zero (implying that the cell is carrying exactly $\Delta I$ less current than the $N^{th}$ cell), that cell's reference voltage will become permanently frozen. Thus, if the rate of change of a cell's reference voltage *ever* goes to zero (as determined in **(17)**), that cell's reference will be frozen permanently at that value. Furthermore, because current differences among cells are not sensitive to changes in the output voltage, the current-sharing dynamics are decoupled from the load dynamics. As a result, once current balance has been established among cells, it will be permanently maintained and cannot be disturbed by load changes.

The preceding discussion of large-signal behavior is valid for cases where the cell output resistances do not change with operating point. However, in many systems, the cell output impedances are resistive but vary with load. In the load-varying output resistance case, the cell with the highest base reference voltage will still permanently act as the master, and the small-signal dynamics about an operating point can still be easily evaluated. However, for large-signal behavior there is some dissimilarity. When the cell output resistances vary across load, the difference between the $j^{th}$ cell's current and the $N^{th}$ cell's current (which appears in **(17)**) is a function of the output voltage. To see this, consider Fig. 6. Figure 6(a) shows the difference in cell currents for two different operating points when the output resistances are identical and constant with load current. As can be seen in the figure (as well as from the result of **(19)**), the difference between cell currents does not depend on output voltage. However, as shown in Fig 6(b), the difference in cell currents does depend on the output voltage when the resistances are identical but load-varying.

This fact can have a strong impact on the current-sharing behavior of a parallel system using this control method. Consider the two-cell case. The control law **(17)** drives the non-dominant cell reference voltage until the cell operates at a current $\Delta I$ below that of the dominant cell (assuming that it does not hit its adjustment boundary first). If the cell output resistances change heavily with load, the voltage reference difference required to support this $\Delta I$ difference is small where the output resistances are low, and large where the output resistances are high. This means

that the non-dominant reference needs to re-adjust under different loading conditions, and that significant current imbalances can occur whenever the loading condition changes from an operating point where the output resistances are high to an operating point where the output resistances are low. This contrasts with the case of constant output resistances, in which the current-sharing dynamics are decoupled from the output dynamics even for large-signal disturbances, and current sharing is permanently maintained once established.

## V. UC3907 Experimental Example

To verify the conclusions of the previous section, we analyze a two-cell system utilizing UC3907 load-sharing IC's, and compare the analytical predictions to experimental results. Each cell is a low-power linear regulator whose reference voltage is derived from the adjusted internal reference of the UC3907. A cell is constructed using a simple op-amp circuit connected to a UC3907 which generates a no-load cell output voltage that is exactly twice the UC3907 adjusted internal reference voltage (i.e. 4.0-4.2 V). Each cell has an output resistance of 4.7 Ω (due to the current-sense resistor at the cell output) and can deliver a full-load current of 30 mA. The two-cell system has a 10 μF output filter capacitance, and drives an *R-L* load, where $L$ = 1.4 mH.

Analytical predictions based on the approach of Section I indicate that the "active" references respond with time constants

$$\tau_j = \frac{1}{GK_j} \qquad (20)$$

while the poles associated with the load are at

$$s = -\left[\frac{R_L}{2L_L} + \frac{NG}{2C_L}\right] \pm \sqrt{\left[\frac{R_L}{2L_L} + \frac{NG}{2C_L}\right]^2 - \frac{1 + NGR_L}{L_L C_L}} \; . \qquad (21)$$

The poles in **(21)** correspond (not surprisingly) to those of the circuit of Fig. 1 with all voltage sources fixed.

The gain of the load-sharing compensation integrator, $K_j$, can be computed as the product of the current-sense resistor value, the current sense amplifier gain (20), the adjustment amplifier transconductance (0.003), the internal gain (0.057), and the external gain (2), all divided by the compensation capacitor value. The 4.7 μF compensation capacitor used in the prototype system yields a gain $K_j$ of approximately 6857 V/(A-s), with a significant amount of variability (3690 to 10800 V/(A-s)) due the uncertainty in parameters such as the adjustment amplifier transconductance.

Given this value of $K_j$, **(20)** predicts first-order current-sharing adjustment dynamics with a time constant of approximately 685 μs. Figure 7 shows the transient response of the cell output currents when a short on the current-sharing line is removed (with $R_L$ = 3.3 kΩ). When the short is removed, the references of both cells are at their lowest (base) values. The reference of the master remains at this value when the short is removed, while the other cell raises its reference voltage to achieve current sharing. The reference adjustment response has a forced component, due to the offset $\Delta I$, as well as a natural component. From the 63% rise time of the response, we estimate a time constant of about 1.2 ms, which is consistent with the predicted dynamics to within the level of parameter uncertainty in the system.

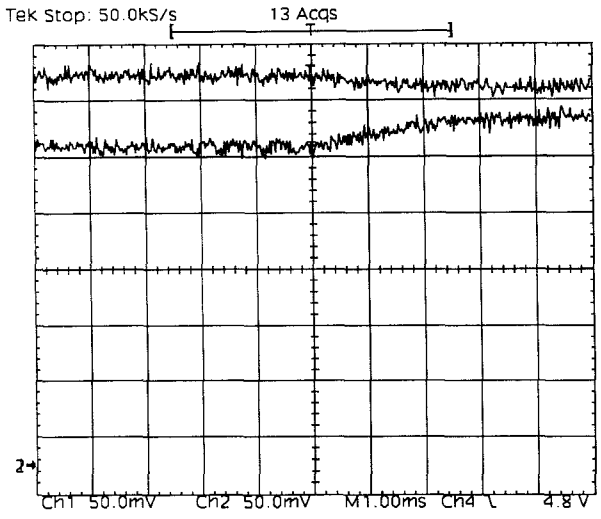


**Figure 7** Transient response of the cell output currents to the removal of a short circuit on the current-sharing line at $t$ = 0. Recorded signals correspond to the outputs of the current-sense amplifiers, with the system operating at a load resistance of 3.3 kΩ.

Figure 8 shows the transient response of the prototype system to load steps between 90 Ω and 1000 Ω. For the load step to 1000 Ω, the system poles are located at -500,000 and -41,000 Np/s (as estimated by the 63% rise times in Fig. 8 (a)), while **(21)** predicts poles at $s$ = -717180 and -42260 Np/s. Similarly, for the load step to 90 Ω, **(21)** predicts pole locations of -60249 and -46590 Np/s. The actual position of one pole (at -66,000 Np/s) is easily estimated from the load resistor voltage response in Fig. 8 (b). However, the other pole location is harder to identify directly, since both poles contribute to the cell current responses and the poles are not widely separated. Nevertheless, comparisons to simulations indicate that the predicted pole location corresponds accurately to the observed response. Thus, the predictions match the observed responses very well. Furthermore, current-sharing is not disturbed by these large load steps, indicating that, as predicted, current-sharing is not affected by changes in output voltage, and the reference adjustment dynamics are decoupled from the output dynamics. What may be concluded from these results is that, under the constraint of resistive output impedances, the dynamics of a system employing the UC3907 load-sharing IC can be accurately predicted.

## VI. Conclusions

The ability to predict the load-sharing dynamics is an important aspect of the design of a cellular converter system. This paper has

addressed the analysis of systems employing nonlinear distributed load-sharing techniques. A methodology has been presented for analyzing nonlinear load-balancing control methods that are linearizable about an operating point. The approach has been applied to a recently-developed load-sharing control technique and compared to experimental results. The paper has also addressed the analysis of the control scheme used in the UC3907 load-sharing control IC, which is not easily handled by linearization in the general case. The dynamics of this control scheme have been established for an important special case, and validated against experimental results.

## ACKNOWLEDGMENTS

The authors would like to gratefully acknowledge the support for this research provided by the Bose Foundation and the Office of Naval Research.

## REFERENCES

[1] L. Walker, "Parallel Redundant Operation of Static Power Converters," *IEEE Industry Applications Society Annual Meeting*, 1973, p. 603-614.

[2] M. Youn and R. Hoft, "Analysis of Parallel Operation of Inverters," *IEEE Industry Applications Society Annual Meeting*, 1976.

[3] T. Kawabata and S. Higashino, "Parallel Operation of Voltage Source Inverters," *IEEE Transactions on Industry Applications*, Vol. 24, No. 2, Mar/Apr 1988, pp. 281-287.

[4] K.T. Small, "Single Wire Current Share Paralleling of Power Supplies," *U.S. Patent 4,717,833*, 1988.

[5] R. Wu, T. Kohama, Y. Kodera, T. Ninomiya, and F. Ihara, "Load-Current-Sharing Control for Parallel Operation of DC-to-DC Converters," *IEEE Power electronics Specialists Conference*, 1993, pp. 101-107.

[6] D. Maliniak, "Dense DC-DC Converters Actively Share Stress," *Electronic Design*, Jan. 21, 1993, pp. 39-44.

[7] M. Jordan, "UC3907 Load Share IC Simplifies Parallel Power Supply Design," *Unitrode Application Note U-129*, Unitrode Corp., Merrimack, NH.

[8] T. Kohama, T. Ninomiya, M. Shoyama, and F. Ihara, "Dynamic Analysis of Parallel Module Converter System with Current Balance Controllers," *1994 IEEE Telecommunications Energy Conference Record*, 1994, pp. 190-195.

[9] T. Kohama, T. Ninomiya, M. Wakamatsu, and M. Shoyama, "Static and Dynamic Response of a Parallel-Module High Power-Factor Converter System with Current-Balancing Controllers," *IEEE Power Electronics Specialists Conference*, 1996, pp. 1198-1203.

[10] D.S. Garabandic and Trajko B. Petrovic, "Modeling Parallel Operating PWM DC/DC Power Supplies," *IEEE Trans. Industrial Electronics*, Vol. 42, No. 5, Oct. 1995, pp. 545-551.

[11] M. Jovanovic, D. Crow, and L. Fang-Yi, "A Novel, Low-Cost Implementation of 'Democratic' Load-Current Sharing of Paralleled Converter Modules," *IEEE Trans. Power Electron.*, Vol. 11, No. 4, July 1996, pp. 604-611.

[12] D.J. Perreault, R. Selders, and J.G. Kassakian, "Frequency-Based Current-Sharing Techniques for Paralleled Power Converters", *1996 IEEE Power Electronics Specialists Conference*, Baveno, Italy, June 1996, pp. 1073-1080.

[13] D.J. Perreault, R.L. Selders, and J.G. Kassakian, "Implementation and Evaluation of a Frequency-Based Current-Sharing Technique for Cellular Converter Systems," *IEEE Africon `96*, Matieland, South Africa, Sept. 1996, pp. 682-686.

[14] R.L. Selders, "A Current-Balancing Control System for Cellular Power Converters", S.M. Thesis, *M.I.T. Department of Electrical Engineering and Computer Science*, Feb. 1996.

[15] V.J. Thottuvelil and G.C. Verghese, "Stability Analysis of Paralleled DC/DC Converters with Active Current Sharing," *IEEE Power Electronics Specialists Conference*, 1996, pp. 1080-1086.

[16] V.J. Thottuvelil and G.C. Verghese, "Analysis and Control Design of Paralleled DC/DC Converters with Current Sharing," *1997 IEEE Applied Power Electronics Conference*, Feb. 1997.

[17] Y. Panov, J. Rajagopalan, and F.C. Lee, "Analysis and Design of N Paralleled DC-DC Converters with Master-Slave Current-Sharing Control," *1997 IEEE Applied Power Electronics Conference*, pp. 436-442, Feb. 1997.

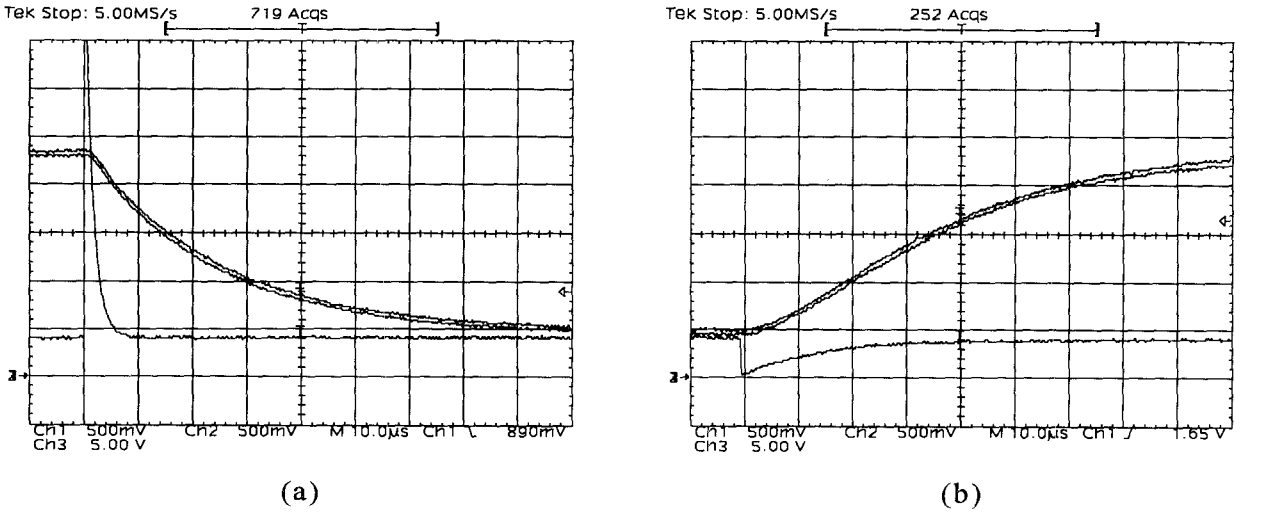


**Figure 8** Transient response of the prototype system output voltage and cell currents to load steps: (a) From 90 Ω to 1000 Ω. (b) From 1000 Ω to 90 Ω. Channels 1 and 2 show the current-sense amplifier outputs, while channel 3 shows the load resistor voltage.